Ecological Modelling 313 (2015) 251–258

Contents lists available at ScienceDirect

Ecological Modelling

journal homepage: www.elsevier.com/locate/ecolmodel

Identifying bloom origins of the toxic dinoflagellate *Karenia brevis* in the western Gulf of Mexico using a spatially explicit individual-based model

Darren W. Henrichs [a], Robert D. Hetland [a], Lisa Campbell [a,b,*]

[a] Department of Oceanography, Texas A&M University, College Station, TX 77843, United States
[b] Department of Biology, Texas A&M University, College Station, TX 77843, United States

ARTICLE INFO

Article history:
Received 9 March 2015
Received in revised form 18 June 2015
Accepted 20 June 2015

Keywords:
Harmful algal bloom
HYCOM
Texas
Diel vertical migration
Individual-based model
Swimming behavior

ABSTRACT

Harmful algal blooms caused by *Karenia brevis* result in large fish kills, human respiratory irritation, and shellfishing closures in affected areas. Most previous work on bloom formation in the Gulf of Mexico has focused on the west coast of Florida. To investigate the origin of bloom-forming cells along the coast of Texas, potential distributions of cells during two bloom years (2009, 2011) and one non-bloom year (2010) were examined using a spatially explicit, individual-based model of *K. brevis*. The model incorporates a previously developed model of dinoflagellate vertical migration and utilizes observed data (field samples of cell concentrations, photosynthetically active radiation) and modeled environmental output (salinity, temperature, current velocities) from a hydrodynamic model. Running the model in reverse showed that cells near the coast of Texas during early fall originate from the southern Gulf of Mexico in bloom years and from the northern Gulf of Mexico in the non-bloom year for the three years studied. Identification of a southern origin for bloom-forming cells provides a target area for increased sampling in order to provide early warning of potentially harmful algal blooms of *K. brevis*.

1. Introduction

Harmful algal blooms formed by the dinoflagellate *Karenia brevis* have occurred in the Gulf of Mexico (hereafter Gulf) for at least several hundred years and likely longer (Magaña et al., 2003). Blooms of *K. brevis* occur almost every year on the west coast of Florida, but infrequently near the coast of Texas. The factor(s) responsible for this difference are not known. The harmful impacts of blooms (i.e., fish kills, respiratory irritation, and shellfish toxicity resulting in closures of shellfishing) can result in millions of dollars of lost revenue for local economies (Hoagland et al., 2002). *K. brevis* is a species tolerant of a wide range of light intensities, salinities, and temperatures (Brand et al., 2012) and has been found throughout the Gulf at low background concentrations (1–1000 cells L^{-1}; Tester and Steidinger, 1997). In contrast to other dinoflagellates (e.g., *Alexandrium* spp.), there is no known seed bed of *K. brevis* and resting stages (e.g., cysts) have not been conclusively identified, raising the question: where do bloom-forming cells off the coast of Texas originate?

On the west Florida shelf, initiation of blooms typically begins ~18–74 km offshore and at depth (Steidinger et al., 1998). These offshore blooms can then be concentrated onshore where their harmful effects are often observed. The frequency with which blooms occur near Florida has resulted in extensive research on blooms and bloom development in this region (e.g. Hu et al., 2008; Milroy et al., 2008; Robbins et al., 2006; Vargo et al., 2004) but research into the development of blooms near Texas has remained minimal (Hetland and Campbell, 2007; Stumpf et al., 2008; Thyng et al., 2013). Previous work revealed no genetic differentiation among blooms from Florida and blooms from Texas and it was hypothesized that bloom-forming cells in Florida and Texas originate from the same source yet the location of the source population remained unknown (Henrichs et al., 2013). Blooms of *K. brevis* off the coast of Texas appear to be the product of widely dispersed cells accumulating by physical concentration (Hetland and Campbell, 2007; Stumpf et al., 2008). The combination of low background cell concentrations and the physical accumulation of cells suggests blooms could occur randomly throughout the year; however, this is not the case. Blooms of *K. brevis* typically initiate from late summer through fall and cells are often not observed above background levels during the rest of the year (Campbell et al., 2013; Magaña et al., 2003; Tester and Steidinger, 1997). Stumpf et al. (2008) hypothesized that blooms of *K. brevis* occurring off the coast of Texas might

* Corresponding author at: Department of Oceanography, Texas A&M University, College Station, TX 77843, United States. Tel.: +1 979 845 5706; fax: +1 979 845 6331..
E-mail address: lisacampbell@tamu.edu (L. Campbell).

http://dx.doi.org/10.1016/j.ecolmodel.2015.06.038
0304-3800/

have initiated in Mexican waters near the southwestern side of the Bay of Campeche and been advected northward. Further support for a southern origin of *K. brevis* cells was given by Thyng et al. (2013), who found modeled surface drifters released in the region near Port Aransas, TX predominantly originated from the southern region of the Texas coast in years when blooms of *K. brevis* occurred. However, surface drifters may not capture critical aspects of bloom distributions. Like many dinoflagellate species, *K. brevis* vertically migrates and blooms of *K. brevis* are known to form at depth (Steidinger et al., 1998). Janowitz et al. (2008) used the behavioral model of Liu et al. (2001a,b) in a three-dimensional simulation of vertically migrating cells of *K. brevis* and demonstrated that wind-driven currents could drive a single column of cells to become spatially distinct populations depending on their initial vertical distribution. Inclusion of vertical migration behavior into models of *K. brevis* distributions could provide more insight into bloom origins and formation. Identification of a region where cells are known to originate is important for early warning systems and would permit further study of the life history stages of this species (including a cyst stage, if any). To investigate the origin of blooms along the coast of Texas, we developed a spatially explicit, individual-based model (IBM) of *K. brevis* that combines modeled output from a hydrodynamic model with a behavioral model of vertical migration for *K. brevis* (Liu et al., 2001a,b). The model can be run forward or backward in time. By running the IBM backwards in time and inserting cells into the model based on field observations from actual bloom events off the coast of Texas, we identified a region from which bloom-forming cells are likely to originate.

2. Methods

2.1. Input data acquisition and preprocessing

2.1.1. Hydrodynamic model

Hourly snapshot files from the 1/25° Gulf of Mexico analysis of the hybrid coordinate ocean model (HYCOM) for the years 2009, 2010, and 2011 were downloaded from the FTP data server (ftp://ftp.hycom.org/datasets/GOMl0.04/expt_31.0/data/). The model outputs for temperature, salinity, u, v, and mixed layer depth were utilized from all grid points between 18.09 and 30.76°N (latitude) and −98.00 to −86.03°W (longitude) in the top 17 depth layers (0, 5, 10, 15, 20, 25, 30, 40, 50, 60, 70, 80, 90, 100, 125, 150, 200 m) of the HYCOM output (Fig. 1).

2.1.2. MODIS data

Daily photosynthetically active radiation (PAR) data (~4 km resolution) from the MODIS sensor on NASA's Aqua and Terra satellites was downloaded (http://oceandata.sci.gsfc.nasa.gov/) and combined into a single input file for each year (2009, 2010, 2011). If PAR data for a grid point were available from both satellite files, the PAR values were averaged together. Because the locations of the grid points from the HYCOM data and MODIS data differed, the MODIS data were re-gridded based on latitude and longitude to match the model grid from HYCOM. Data for the new grid points were linearly interpolated from the data at the original grid points.

2.1.3. K. brevis *sample data*

Information about the location, cell concentrations, and date/time of sample collection was obtained from Texas Parks and Wildlife Department (TPWD) and the Imaging FlowCytobot (IFCB) deployed at Port Aransas, TX (Campbell et al., 2013). When depth information was unavailable, it was assumed the sample was taken near the surface and a depth of one meter was used.

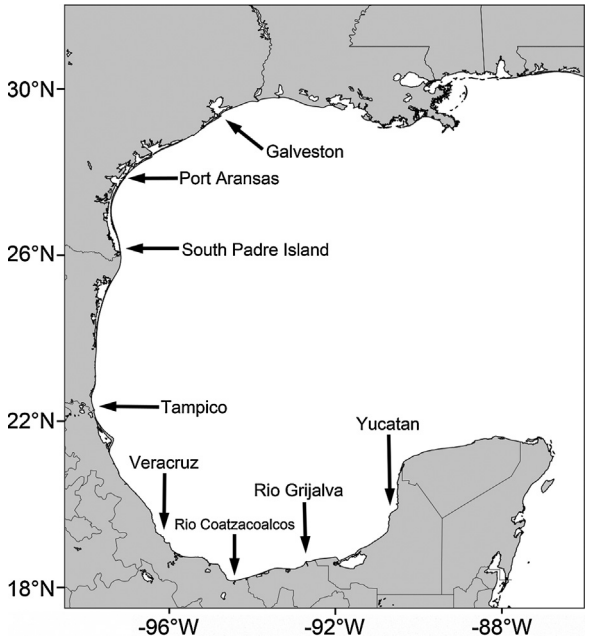

Fig. 1. Western Gulf of Mexico model domain. Arrows indicate locations where blooms of *Karenia brevis* have been known to occur historically.

2.1.4. Nutrient concentration

The only nutrient considered in the model was nitrate. Field measurements of nitrate concentrations throughout the Gulf of Mexico are few and instead, a simple nutrient gradient increasing with depth was used throughout the model domain. The nutrient concentration equation of Liu et al. (Eq. 12, 2001b) was modified so that the nutricline depth at a given location in the model was set to be the depth of the mixed layer (see Section 2.1.1 above) at that same location. The nutrient concentration at the surface was set to a background level of 0.05 μM, a similar background level used by Liu et al. (0.10 μM, 2001b) in their model and within the range observed off the coast of Texas during cruises in the summer of 2013 and 2014 (S. DiMarco pers. comm.), and increased with depth. Nitrate concentration at a given location was fixed during a time step and nutrient uptake by individuals did not reduce nitrate concentration in the environment.

2.2. Individual-based model

A very brief description of the model used for vertical migration of the individuals is given below. A fully detailed description of the IBM following the ODD protocol (Grimm et al., 2010), including model equations, can be found in the Appendix.

2.2.1. Movement of individuals

Movement of individuals in the vertical (z) domain is driven solely by the vertical migration of the individuals while movements in the horizontal (x,y) domains are driven solely by the current velocities provided by the hydrodynamic model (i.e. individuals do not 'swim' horizontally but are instead passively carried by currents). This model simplification was made to highlight the role of diel vertical migration (DVM) on the distribution of individuals. A discrete, three minute time step was used in all model runs (i.e. individuals' locations were updated 480 times per model day). Equations were processed following the Euler method and the values of an individual's internal variables at each time step were determined only by the internal and external (environmental) variables from the previous time step. During forward runs, individuals were stepped forward in time according to the current velocities

Table 1
State variables for a cell.

Variable	Potential range[a]	Value in Liu et al. (2001a)[b]
Cell ID	0–?	n/a
Parent cell	0–?	n/a
Cell origin (start location)	Variable	n/a
Culture	True/false	n/a
Ready to divide	True/false	n/a
Division threshold (Carbon)	90% of carbon max	90% of carbon range
Division threshold (Nitrogen)	95% of nitrogen max	23.3 pmol
Internal carbon (maximum)	0–120.0 pmol	90.0 pmol
Internal carbon (minimum)	0–75.0 pmol	36.0 pmol
Internal carbon (current)	0 – Carbon max	36.0–90.0 pmol
Internal nitrogen (maximum)	0–40.0 pmol	23.3 pmol
Internal nitrogen (minimum)	0–20.0 pmol	6.32 pmol
Internal nitrogen (current)	0 – Nitrogen max	6.32–23.3 pmol
Salinity preferred	10.0–40.0	n/a
Salinity acclimated	Variable	n/a
Salinity stress	0–1.0	n/a
Temperature preferred	15.0–40.0 °C	n/a
Temperature acclimated	Variable °C	n/a
Temperature stress	0–1.0	n/a
Daylength	Variable	12 h
Cell x location	Variable	n/a
Cell y location	Variable	n/a
Cell z location	Variable	n/a

[a] ? indicates the maximum value is not limited.
[b] n/a indicates the variable was not included in Liu et al. (2001a).

and diel vertical migration distance given from the model. During reverse runs, the current velocities and swimming direction are reversed (by inverting the sign of velocity or swimming direction). Turbulent mixing was not included in the present work but see Appendix for its application.

2.2.2. Addition of new individuals

Individuals were created by randomly assigning combinations of physiological parameters (e.g. ideal salinity range, ideal temperature range) to each individual (Table 1). These individuals were then inserted into the model at locations (latitude, longitude, depth) specified before each run and included field sampled bloom events and hypothesized regions of origin. Individuals were inserted at the same time and location for replicate runs and only the combination of physiological parameters in each individual varied among runs. All new individuals were inserted at the same time step each model day and individuals were only added once per model day. Varying combinations of physiological parameters were used to mimic the physiological (and genetic) diversity observed in both laboratory cultures and blooms in the field and, when presented with identical environmental conditions, resulted in responses that varied slightly among individuals.

2.2.3. Diel vertical migration

Individuals swim up or down depending on internal biochemical needs following the behavioral model of Liu et al. (2001a,b). The model developed by Liu et al. (2001a) was designed to reproduce both the vertical distribution of cells and the intracellular biochemical state of those cells based on a laboratory mesocosm experiment. The need for energy (carbon) will cause cells to swim upward to increase the photosynthetic rate and the need for nutrients (nitrate) will cause cells to swim downward (or upward depending on the nutrient gradient) to access higher nutrient concentrations. Carbon is gained by photosynthesis and lost to cellular respiration and when a cell divides. The model uses a simple nutrient concentration gradient with low (background) concentrations at the surface and increasing concentrations with depth with a nutricline occurring at the mixed layer depth. The time of day, nutrient concentration, salinity, temperature, and amount of light available at an individual's depth are all evaluated to determine how much carbon is integrated through photosynthesis and how much nitrate was taken up during each time step (see Appendix for full details). Each individual then determines whether to swim up or down based solely on its present intracellular carbon and nitrate concentrations. The individual is then moved vertically according to the swimming rules given by Liu et al. (2001b) (see also Appendix) and horizontally according to the current velocities. This process is completed once during each time step.

2.3. Test cases

We focus here on three particular years: two years when large blooms of *K. brevis* occurred in Texas (2009, 2011) and one year when no bloom occurred (2010). The IBM was tested using both forward and reverse runs. The reverse model runs were used to highlight differences between bloom years and non-bloom years. Reverse runs incorporating real sample data were further used to identify the likely origin(s) of bloom-forming cells. Forward model runs were used to verify whether cells originating from a region identified in the reverse runs could indeed be transported to the coast of Texas, as observed. Unless otherwise stated, reproduction and death were turned off for all model runs to reduce the amount of random variation in the results from each run and focus on physical conditions of bloom transport. Thus, if the internal carbon (C) and nitrogen (N) stores for an individual reached the thresholds for reproduction, the internal C and N were reduced as though the individual had reproduced (following the unequal daughter strategy of Liu et al., 2001a) however, no new individual was created. If the internal C for an individual fell below the minimum value for that individual, the internal C was set equal to the individual's maximum (minimum) value of C during reverse (forward) runs. However, if a cell left the model domain (advected east) it was removed from the simulation. A brief summary of the settings for each simulation is given in Table 2.

2.3.1. Idealized model setup

A single individual in a static environment (constant salinity, temperature, nutrient concentration, day length) was simulated for 60 model days under three different light scenarios: a 12:12 h light:dark (12L:12D) cycle, constant dark (0L:24D), and constant light (24L:0D) to confirm the swimming behavior and photosynthesis submodels were performing properly. In a laboratory setting under a 12L:12D cycle (commonly used for *K. brevis* cultures), a cell should swim up while light is available (unless its internal C is full) and down when dark (unless its internal N is full or internal C is too low) based on the swimming rules given in Liu et al. (2001b).

Table 2
Settings for various model runs..

Options	Reverse runs (artificial data)	Reverse runs (field sample)	Forward runs	Forward runs (DVM test)
Cell death	No	No	No	Yes
Cell division (growth)	No	No	No	Yes
Mutation	Yes[a]	Yes[a]	Yes[a]	Yes[b]
Mutation rate	0.1	0.1	0.1	0.1
Population size (max.)	100,000	100,000	100,000	100,000
Length of run	160 days	160 days	100 days	100 days
Initial # of cells	0	0	5000	5000

[a] Mutation was allowed during the initial creation of cells at the beginning of a simulation run.
[b] Mutation was allowed at the beginning of a simulation run and each cell division event.

In a constant light scenario, a real cell should fill its internal C and swim down seeking increased nutrient concentrations. The constant availability of light could allow the cell to remain deeper in the water column, seeking a depth that optimizes the rates of photosynthesis and nitrate uptake. In a constant dark scenario, a real cell should use up all available internal C (energy) and swim upward seeking light to photosynthesize, where it would likely die due to a lack of C. Testing of the model swimming behavior required a small modification in order to keep the simulation going for 60 model days: if the internal C fell below the critical threshold (i.e. cell died), the internal C value was reset to the minimum threshold for the cell.

2.3.2. Reverse runs

To determine where bloom-forming cells originated, we ran several model runs in reverse. Cells were placed into the model at locations where and when they were known to occur and run backwards in time to observe the trajectory that cells took in order to end up at the Texas coast. All reverse runs began on Julian day 338 (the last date of a field sample from bloom year 2009) and ran until Julian day 178 (4 Dec to 27 Jun). Three sample locations in Texas were chosen for the initial reverse runs based on geographic spacing and past occurrence of blooms (South Padre Island, Port Aransas, and Galveston; Fig. 1). Cells were added twice weekly at each of the three locations from 3 Dec to 24 Sep, a time span within the bloom periods of 2009 and 2011. Three independent runs for each year were simulated and the results from each year were aggregated. For reverse runs incorporating real sample data, cells were added to the simulation based on field sample data. In order to avoid biasing the simulation distributions with cells from a single, dense sample, cell concentrations for each field sample were limited to a maximum of 25 cells. Running the model in reverse required several elements of the swimming model to be modified and those changes are detailed here. All current velocities (u, v) were reversed by inverting the sign of the velocity value. Because the amount of carbon incorporated from photosynthesis and the amount of nitrate taken up by the cell during each time step would normally be added to the cell's internal stores, in all reverse runs these were instead subtracted from the cell. The decision to swim up or down and at what speed was then calculated based on the reduced values of internal carbon and nitrogen. The swimming direction chosen by each cell was reversed while swimming speed remained the same.

2.3.3. Forward runs

Forward runs were used to verify that cells originating from a region indicated by the reverse runs would in fact travel to the coast of Texas during bloom years and not during the non-bloom year. All forward runs began on Julian day 182 and ended on Julian day 282 (1 Jul to 9 Oct). The start date was arbitrarily chosen to be July 1 for the forward runs and the simulation ran for 100 days. Individuals were only added to the simulation at the start of each model run. For each model run, 5000 cells were added to the area shown in Fig. 2A.

2.3.4. Impact of diel vertical migration

Forward runs were also used to examine the effect of including DVM in the model versus modeling cells as surface drifters or as randomly migrating cells. Again, individuals were only added to the simulation at the start of each model run. For each model run, 5000 cells were added to the area shown in Fig. 2A. Reproduction and death were both allowed during these runs to see what differences in cell growth rates and distributions, if any, were obtained by including DVM. Each run was simulated for one model year (10 Apr 2009–10 Apr 2010).

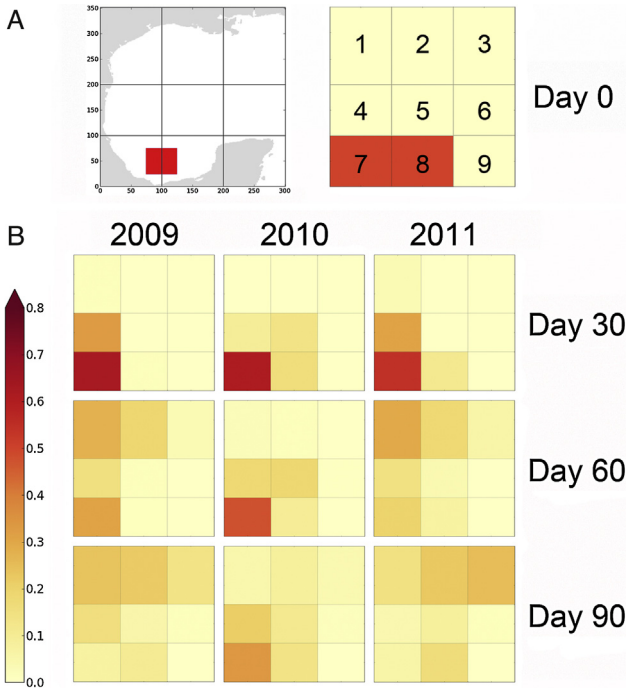

Fig. 2. Heat maps of cell distributions from model runs in forward time. The western Gulf of Mexico was divided into nine regions (boxes 1–3 are extended north to include Galveston Bay, however, this extension mainly incorporates land). All runs were initialized with cells in the southern Gulf of Mexico between boxes 7 and 8. Cells reached the coast of Texas earlier and in higher numbers for the two bloom years (2009, 2011) compared to the non-bloom year (2010). (A) Starting cell locations (left) and heat map distribution (right) for all runs. (B) Heat maps of cell distributions at thirty day intervals. Color of each box indicates proportion of total population present.

3. Results

3.1. Evaluation of idealized model

Given the model rules for swimming behavior, the swimming patterns observed from the three different light scenarios were similar to what would be expected in a laboratory culture of cells under the same conditions. The constant dark scenario resulted in the cell dying numerous times during the simulation, similar to what is expected for a photosynthetic organism (Fig. 3A). The 12L:12D scenario resulted in a repeated pattern of vertical swimming with the final depth of the cell (after acclimating to the environment) between 15 and 19 m (Fig. 3B). The single cell maintained a mean depth of 14.9 m ± 3.3 m (mean ± SD) and divided nineteen times during the 60-day simulation (growth rate = 0.31 div day^{-1}), well within the range of growth rates observed for *K. brevis* in the lab (0.09–0.36 div day^{-1}; Errera et al., 2010; Magaña and Villareal, 2006) and the field (~0.06–0.79 div day^{-1}; Van Dolah et al., 2008). The growth rate under constant light increased by more than half compared to the 12L:12D scenario. However, this result is likely due to the fixed chlorophyll content of cells in the model. This renders the cells incapable of adjusting their chlorophyll content in response to lower or higher light and produces increased photosynthetic activity under constant light and ultimately, a higher growth rate. While the response to constant light in the model may not be realistic, in a field environment a cell will never be exposed to 24 h of continuous light. Based on the swimming behavior and growth rate of the simulated cell under 12L:12D conditions, no major problems with the individual-based implementation of the Liu et al. (2001a,b) model were identified and we proceeded to use the IBM in the reverse and forward simulation runs.

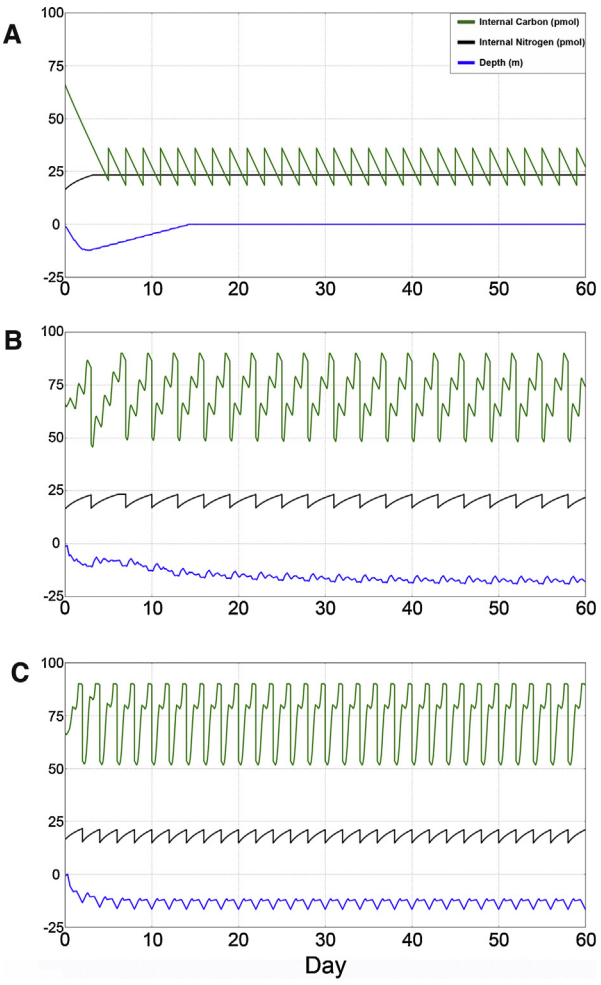

Fig. 3. Swimming behavior of a single cell in a static environment (salinity, temperature, nutrient concentration) under three different light scenarios: (A) 24-h dark, (B) 12L:12D, (C) 24-h light. Vertical lines in the carbon (green) and nitrogen (black) indicate timepoints where carbon/nitrogen was either added because the cell died (A) or removed because the cell divided and lost resources to the daughter cell (B, C).

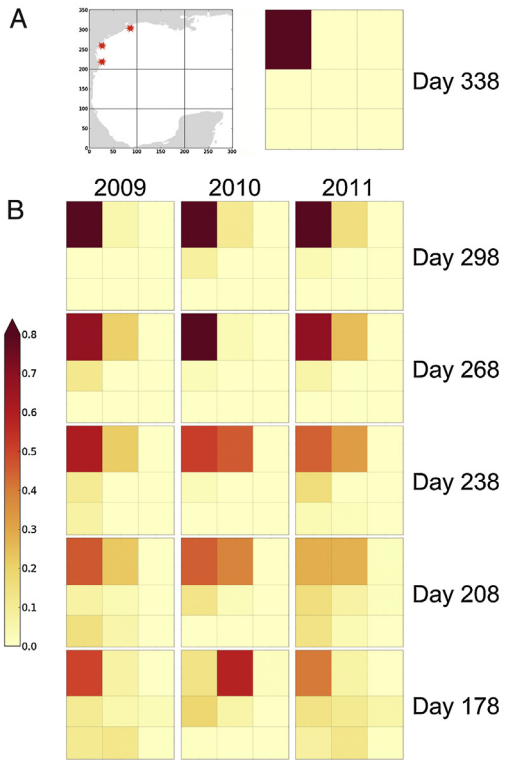

Fig. 4. Heat maps of cell distributions from model runs going backwards in time (reverse runs). The grid regions are as in Fig. 2. (A) Starting cell locations and distributions. During reverse runs, cells were repeatedly inserted at three locations on the coast of Texas (indicated by red stars): Galveston, Port Aransas, and South Padre Island. (B) Heat maps of cell distributions at thirty day intervals. Color of each box indicates proportion of the total population present. Though all cells were inserted off the coast of Texas (box 1), the distribution of cells differs between bloom years (2009, 2011) and the non-bloom year (2010). During bloom years, a higher proportion of cells was found in the southern Gulf of Mexico (boxes 7, 8) at the end of the model runs when compared to the non-bloom year.

3.2. Reverse runs

The reverse simulation runs using artificial data permitted a comparison between bloom years and a non-bloom year and notable differences in the summarized distributions of cells were observed (Fig. 4). At the end of the simulation runs for years 2009 and 2011, a large proportion (~40%) of cells remained in box 1 while boxes 7 and 8 combined to yield ~25% of the cells (Fig. 4B). The non-bloom year, 2010, had only ~16% of the cells remaining in box 1 and ~11% of the cells were located in boxes 7 and 8 (Fig. 4B). At the end of the simulation run for the non-bloom year, the majority of cells (~54%) were located in the northern Gulf with more than half of the total cells near the coast of Louisiana. This was in stark contrast to the bulk of cells remaining near the coast of Texas or that moved south along the Mexican coastline during bloom years. In both 2009 and 2011, less than 3% of cells were located in box 2 at the end of the run. When cells were added based on real sample data, the distribution of cells at the end of the simulation runs was similar to those using artificial data above (Tables S1 and S2). For simulation runs of both 2009 and 2011, a smaller proportion of cells remained in box 1 when compared to the runs using artificial sample data because the distribution of cells from field samples was not equal. The number of samples from a geographic location and cell concentrations among field samples varied greatly. The distribution of cells from 2009 differed between artificial data and real data partly because no cells of *K. brevis* were found in samples collected near Galveston, Texas during that year. Full information about cell distributions can be found in Tables S3–S5. While it is possible that cells remaining near the coast of Texas did in fact originate from that region, it is more likely a byproduct of the near coast current velocities in the HYCOM model. The barrier islands along the coast of Texas are not well resolved by the hydrodynamic model and near shore current velocities may not be accurately represented (Fig. 2A). Despite this, notable differences were still observed between the distributions of cells in bloom years versus non-bloom years and appear to be a result of differences in the current fields during those years.

3.3. Forward runs

Forward simulation runs indicated cells could be transported from the southern region of the western Gulf to the coast of Texas and again, measurable differences in the distributions of cells were detected between bloom years and non-bloom years. Cell distributions after 30, 60, and 90 days can be found in Fig. 2. Individual cell distributions after 60 days from one run for each year are shown in Fig. 5. More than a third (>33%) of the cells were located in box 4 after 30 days during bloom years while ~14% of cells were in box 4 in the non-bloom year (Fig. 2B). After 90 days, >50% of the cells were located in boxes 1, 2, and 3 during bloom years but only ~20% of cells were in the same locations during the non-bloom year (Fig. 2B). The majority of cells during the non-bloom year remained in boxes 7 and 8. While our simulated "blooms" are modeled as

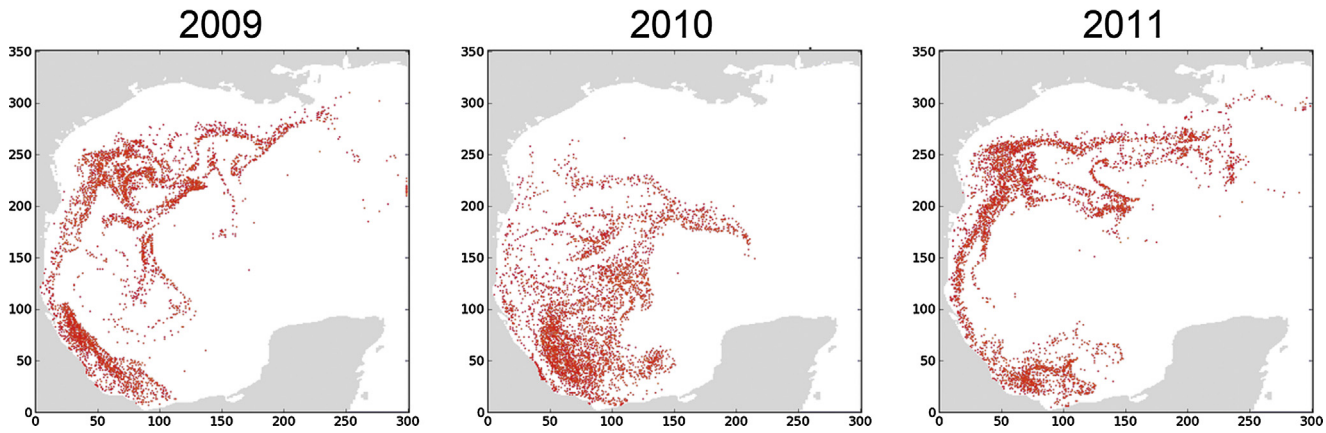

Fig. 5. Distributions of individual cells after 60 days from a single model run in forward time for each year highlight the differences between bloom years (2009, 2011) and the non-bloom year. Each red dot represents a single individual cell from the model.

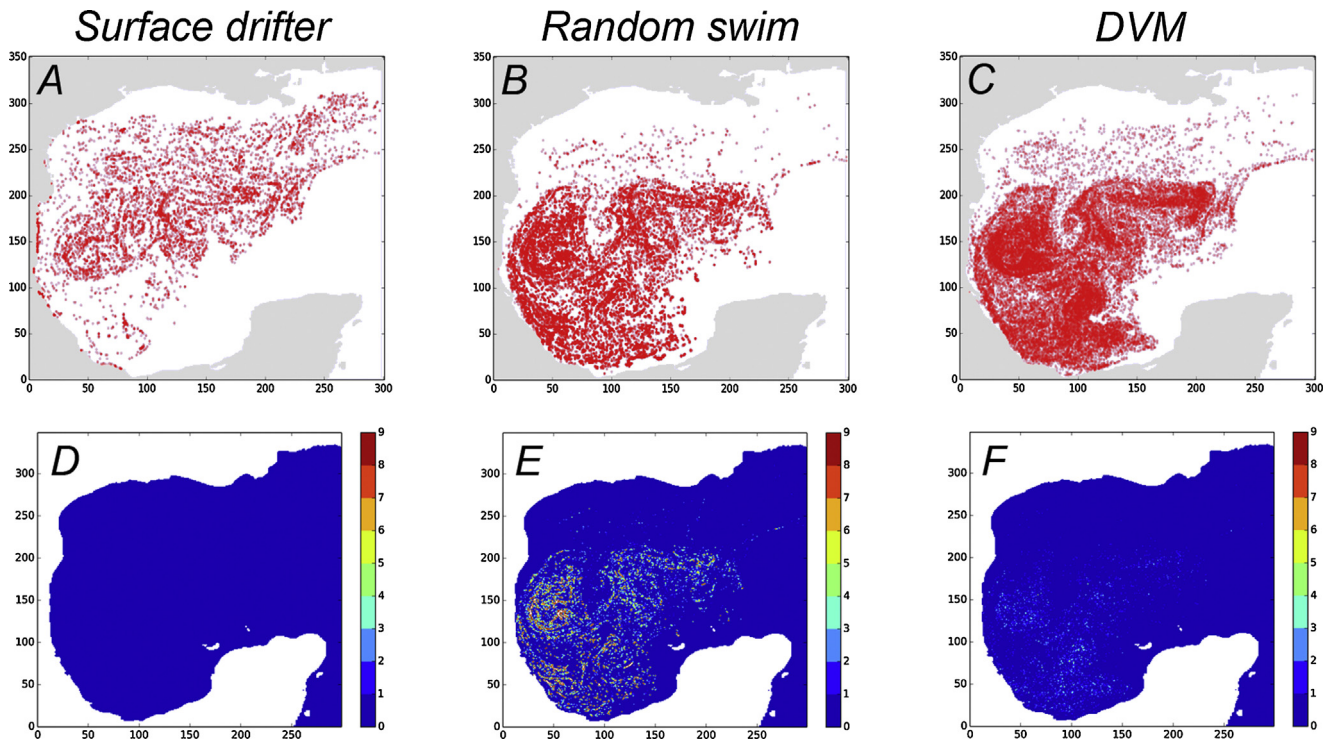

Fig. 6. Distributions of individual cells after one model year (10 Apr 2009–10 Apr 2010) under three different swimming scenarios. The vertically integrated geographic distribution of cells, represented by red dots, are displayed in the top row. The bottom row shows cell concentrations at 25 m depth. Scale bars indicate the number of individuals present. (A, D) Surface drifter scenario: cells are held at the surface and cannot swim vertically. No cells are observed at 25 m depth. (B, E) Random swimming scenario: cells randomly swim up or down and at random speeds. Aggregations of cells are observed at 25 m depth (and other depths). (C, F) Diel vertical migration scenario: cells are allowed to vertically migrate at varying speeds dependent upon internal physiological needs. Cells are not aggregated at 25 m depth (or other depths) and are more evenly distributed vertically.

discrete events, with no cells being present anywhere else in the model domain at the start of a run, in reality, cells are found throughout the Gulf at low levels (Tester and Steidinger, 1997). Full distribution information can be found in Tables S6–S8.

3.4. Impact of diel vertical migration

Each swimming scenario was run one time to demonstrate the differences between scenarios. The surface drifter model run showed lower overall growth (growth rate = 0.20 div day^{-1}). The distribution of cells was more to the north and many cells were advected out of the model domain (Fig. 6A). The remaining two model runs, incorporating random swimming and DVM behavior, resulted in cells remaining within the model domain at high abundance. Overall growth rates for random swimming (growth rate = 0.39 div day^{-1}; Fig. 6B) and DVM (growth rate = 0.36 div day^{-1}; Fig. 6 C) were higher but still similar to culture and field values after one year. While the spatial distributions of cells from the DVM and random swimming runs were similar, differences were observed upon closer inspection of the vertical distributions. The model run incorporating random swimming behavior resulted in dense aggregations of cells at various locations throughout the model domain because newly divided cells did not actively swim toward the surface (Fig. 6E). The majority of cells in these aggregations were from the same lineage and likely the product of repeated divisions (data not shown). The model run incorporating DVM behavior resulted in a similar spatial distribution of cells but the vertical distribution was more diffuse and dense

aggregations at a depth were not observed (Fig. 6F). The inclusion of DVM behavior caused a stable presence of cells in the southern Gulf, the same region from which bloom-forming cells originate according the reverse runs (above). Though cells were present throughout the model domain, cell numbers were reduced in the northern Gulf during the winter months due to colder water temperatures. The lack of swimming in the surface drifter run resulted in no cells at the 25 m depth (Fig. 6D)

4. Discussion

4.1. Reverse runs

The reverse simulation runs based on actual sample data showed many cells originated from the southern Gulf in bloom years (2009, 2011), which is consistent with the results of Thyng et al. (2013) who reported a southern origin for simulated surface drifters (as a proxy for cells of *K. brevis*) during bloom years. The presence of cells of *K. brevis* in the southern Gulf is supported by historical records of blooms of *K. brevis* along the Mexican coast and includes a bloom of *K. brevis* in September of 2011 off the western coast of the Yucatan peninsula (Fig. 1; Magaña et al., 2003; Hernández-Becerril et al., 2007; Soto et al., 2012; Soto Ramos, 2013). The southern extent of the model domain used by Thyng et al. (2013) was limited to the middle region of the western Gulf of Mexico, south of the border between the United States and Mexico. The extension of the model domain to encompass the entire southern Gulf has permitted us to track cells further south, thereby identifying areas of potential origin and possible targets for a sampling program that could provide early warning for potential harmful algal blooms.

4.2. Forward runs

Thyng et al. (2013) found that a weak downcoast mean alongshore wind velocity for the month of September was required for bloom formation along the coast of Texas. This result was in agreement with the results of Hetland and Campbell (2007) in showing that downwelling at the coast can result in a coastal aggregation of spatially dispersed cells. The model results in this paper suggest subsurface cells are advected north toward the coast of Texas during the summer months and can provide an above background concentration seed population for a fall bloom. The mean alongshore wind velocity for September 2010 was only slightly greater than the threshold of $-1.65\ m\ s^{-1}$ determined by Thyng et al. (2013) so the potential impacts from the lack of a seed population from the southern Gulf in 2010 remain unknown (see Fig. 2 in Thyng et al., 2013).

4.3. DVM behavior, model realism, and limitations

The positive effect of including DVM into the model was apparent from the results shown (Fig. 6). The lower growth rate in the surface drifter scenario was due to the inability of cells to access higher nutrient concentrations at depth. Cells took longer to acquire enough nitrate in order to divide and either died (i.e. grazed) or were advected out of the model domain before dividing. The random swimming scenario produced a higher growth rate but also resulted in aggregations of clonal cells at various depths. However, these aggregations are inconsistent with the observed background cell concentrations of *K. brevis* and the high genetic diversity detected among field blooms (Henrichs et al., 2013; Tester and Steidinger, 1997). While cells in the DVM scenario were present throughout the model domain, there was a consistent population of cells in the southern Gulf and from this population, filaments of cells were advected north toward Texas. The constant presence of a population of cells in the southern Gulf lends further support to the idea that this region may be a source region for cells that ultimately form blooms off the coast of Texas. One caveat to these results is the dependence of growth on nutrient availability. A highly simplified nitrate distribution (low concentration at the surface increasing with depth) was used for all model runs but this may not be realistic in all regions of the Gulf (e.g., near the Mississippi river). However, the ability of the cells in the DVM scenario to swim toward higher nutrient concentrations, deeper or shallower, is likely to result in their superior performance (compared to random swimming or surface drifters) in differing nutrient distributions.

The original behavioral model of Liu et al. (2001a) was designed to reproduce the observations of Kamykowski et al. (1998a,b) from a previous mesocosm experiment conducted in a laboratory setting. The effects of temperature and salinity on swimming behavior and growth were not included in the original model but are likely quite important in the field. Temperature and salinity in the western Gulf varies seasonally and can directly impact growth rates of *K. brevis* (Magaña and Villareal, 2006). Sensitivity to temperature and salinity were added to the model presented here in order to provide a cellular response to changing environmental conditions. Stress factors were not quantitatively measured from cultures but were based upon previous observations: quick changes in water temperature resulted in death of cells (R.M. Errera, personal communication) and lack of acclimation to changes in salinity can result in narrower apparent ranges of growth (Brown et al., 2006). Swimming speeds of dinoflagellates can change due to temperature, with increased swimming speeds at increased temperatures for some dinoflagellates (Kamykowski and McCollum, 1986). The swimming speed of *K. brevis* varies among strains but changed very little over the range of temperature where growth occurred (McKay et al., 2006) and therefore temperature-adjusted swimming speed was not implemented in the model.

The assumption that vertical movement of cells is solely a product of vertical migration (i.e. swimming) is an oversimplification. In reality, turbulent mixing can impact cells by either delaying (or denying) a cell from reaching a desired depth or causing it to reach a desired depth faster than expected. We chose to focus on the impact of including DVM into the model and, while mixing is included in the overall model structure, it was not implemented for the model runs presented here. The use of fixed values for internal cellular thresholds is another simplification. Cells modify their behavior based on internal needs and it is possible these needs are changing over time. The impact of these limitations on cell distributions is unknown but the model presented here provides a first step toward identifying the true distributions.

4.4. Conclusions

The present work supports the hypothesis of Stumpf et al. (2008) of a southern origin for blooms near Texas. The conceptual model of Thyng et al. (2013) requiring an input of cells (i.e. a seed population) from the south, in addition to weak downcoast winds, for bloom formation off the coast of Texas is further supported by the present results. When run in forward time, the model can provide short-term forecasts of potential bloom formation, thereby providing an additional early warning tool. Future work should focus on field sampling from the Bay of Campeche region in the southern Gulf in order to confirm our results and potentially provide early warning for potential blooms off the coast of Texas.

Acknowledgements

This work was supported by a grant from the National Oceanographic and Atmospheric Administration/Ecology of Harmful Algal

Blooms program (NOAA/ECOHAB) to L.C. and R.D.H. We would like to thank Karen A. Steidinger for providing information regarding *K. brevis* bloom events in Mexico, Meridith Byrd and Texas Parks and Wildlife Department for providing field sample information from the 2009 and 2011 *K. brevis* bloom events, and two anonymous reviewers whose comments greatly improved this manuscript. This paper is ECOHAB contribution 827.

Appendix A. Supplementary data

Supplementary data associated with this article can be found, in the online version, at http://dx.doi.org/10.1016/j.ecolmodel.2015.06.038

References

Brand, L.E., Campbell, L., Bresnan, E., 2012. *Karenia*: the biology and ecology of a toxic genus. Harmful Algae 14, 156–178.

Brown, A.F.M., Dortch, Q., Van Dolah, F.M., Leighfield, T.A., Morrison, W., Thessen, A.E., Steidinger, K., Richardson, B., Moncrieff, C.A., Pennock, J.R., 2006. Effect of salinity on the distribution, growth, and toxicity of *Karenia* spp. Harmful Algae 5, 199–212.

Campbell, L., Henrichs, D.W., Olson, R.J., Sosik, H.M., 2013. Continuous automated imaging-in-flow cytometry for detection and early warning of *Karenia brevis* blooms in the Gulf of Mexico. Environ. Sci. Pollut. Res. 20, 6896–6902.

Errera, R.M., Bourdelais, A., Drennan, M.A., Dodd, E.B., Henrichs, D.W., Campbell, L., 2010. Variation in brevetoxin and brevenal content among clonal cultures of *Karenia brevis* may influence bloom toxicity. Toxicon 55, 195–203.

Grimm, V., Berger, U., DeAngelis, D.L., Polhill, J.G., Giske, J., Railsback, S.F., 2010. The ODD protocol: a review and first update. Ecol. Model. 221, 2760–2768.

Henrichs, D.W., Renshaw, M.A., Gold, J.R., Campbell, L., 2013. Population-genetic structure of the toxic dinoflagellate *Karenia brevis* from the Gulf of Mexico. J. Plankton Res. 35, 427–432.

Hernández-Becerril, D.U., Alonso-Rodríguez, R., Álvarez-Góngora, C., Barón-Campis, S.A., Ceballos-Corona, G., Herrera-Silveira, J., Meave del Castillo, M.E., Juárez-Ruíz, N., Merino-Virgilio, F., Morales-Blake, A., Ochoa, J.L., Orellana-Cepeda, E., Ramírez-Camarena, C., Rodríguez-Salvador, R., 2007. Toxic and harmful marine phytoplankton and microalgae (HABs) in Mexican coasts. J. Envir. Sci. Health A 42, 1349–1363.

Hetland, R.D., Campbell, L., 2007. Convergent blooms of *Karenia brevis* along the Texas coast. Geophys. Res. Lett. 34, L19604.

Hoagland, P., Anderson, D.M., Kaoru, Y., White, A.W., 2002. The economic effects of harmful algal blooms in the United States: estimates, assessment issues, and information needs. Estuaries 25, 819–837.

Hu, C., Luerssen, R., Muller-Karger, F.E., Carder, K.L., Heil, C.A., 2008. On the remote monitoring of *Karenia brevis* blooms of the west Florida shelf. Cont. Shelf Res. 28, 159–176.

Janowitz, G.S., Kamykowski, D., Liu, G., 2008. A three-dimensional wind and behaviorally driven population dynamics model for *Karenia brevis*. Cont. Shelf Res. 28, 177–188.

Kamykowski, D., McCollum, S.A., 1986. The temperature acclimatized swimming speed of selected marine dinoflagellates. J. Plankton Res. 8, 275–287.

Kamykowski, D., Milligan, E.J., Reed, R.E., 1998a. Biochemical relationships with the orientation of the autotrophic dinoflagellate *Gymnodinium breve* under nutrient replete conditions. Mar. Ecol. Prog. Ser. 167, 105–117.

Kamykowski, D., Milligan, E.J., Reed, R.E., 1998b. Relationships between geotaxis/phototaxis and diel vertical migration in autotrophic dinoflagellates. J. Plankton Res. 20, 1781–1796.

Liu, G., Janowitz, G.S., Kamykowski, D., 2001a. A biophysical model of population dynamics of the autotrophic dinoflagellate *Gymnodinium breve*. Mar. Ecol. Prog. Ser. 210, 101–124.

Liu, G., Janowitz, G.S., Kamykowski, D., 2001b. Influence of environmental nutrient conditions on *Gymnodinium breve* (Dinophyceae) population dynamics: a numerical study. Mar. Ecol. Prog. Ser. 213, 13–37.

Magaña, H.A., Contreras, C., Villareal, T.A., 2003. A historical assessment of *Karenia brevis* in the western Gulf of Mexico. Harmful Algae 2, 163–171.

Magaña, H.A., Villareal, T.A., 2006. The effect of environmental factors on the growth rate of *Karenia brevis* (Davis) G. Hansen and Moestrup. Harmful Algae 5, 192–198.

McKay, L., Kamykowski, D., Milligan, E., Schaeffer, B., Sinclair, G., 2006. Comparison of swimming speed and photophysiological responses to different external conditions among three *Karenia brevis* strains. Harmful Algae 5, 623–636.

Milroy, S.P., Dieterle, D.A., He, R., Kirkpatrick, G.J., Lester, K.M., Steidinger, K.A., Vargo, G.A., Walsh, J.J., Weisberg, R.H., 2008. A three-dimensional biophysical model of *Karenia brevis* dynamics on the west Florida shelf: a look at physical transport and potential zooplankton grazing controls. Cont. Shelf Res. 28, 112–136.

Robbins, I.C., Kirkpatrick, G.J., Blackwell, S.M., Hillier, J., Knight, C.A., Moline, M.A., 2006. Improved monitoring of HABs using autonomous underwater vehicles (AUV). Harmful Algae 5, 749–761.

Soto, I., Hu, C., Steidinger, K.A., Muller-Karger, F., Cannizzaro, J., Wolny, J., Cerdeira-Estrada, S., Santamaria del Angel, E., Tafoya del Angel, F., Alvarez-Torres, P., Herrera-Silveira, J., Allen, J., 2012. Binational collaboration to study Gulf of Mexico's harmful algae. Eos 93, 49–50.

Soto Ramos, I.M., 2013. Harmful Algal Blooms of the West Florida Shelf and Campeche Bank: Visualization and Quantification Using Remote Sensing Methods. Graduate School Theses and Dissertations, http://scholarcommons.usf.edu/etd/4775

Steidinger, K.A., Vargo, G.A., Tester, P.A., Tomas, C.R., 1998. Bloom dynamics and physiology of *Gymnodinium breve* with emphasis on the Gulf of Mexico. In: Anderson, D.M., Cembella, A.D., Hallegraeff, G.M. (Eds.), Physiological Ecology of Harmful Algal Blooms. Springer, New York, pp. 135–153.

Stumpf, R.P., Litaker, R.W., Lanerolle, L., Tester, P.A., 2008. Hydrodynamic accumulation of *Karenia* off the west coast of Florida. Cont. Shelf Res. 28, 189–213.

Tester, P.A., Steidinger, K.A., 1997. *Gymnodinium breve* red tide blooms: initiation, transport, and consequences of surface circulation. Limnol. Oceanogr. 42, 1039–1051.

Thyng, K.M., Hetland, R.D., Ogle, M.T., Zhang, X., Chen, F., Campbell, L., 2013. Origins of *Karenia brevis* harmful algal blooms along the Texas coast. Limnol. Oceanogr. Fluids Environ. 3, 269–278.

Van Dolah, F.M., Leighfield, T.A., Kamykowski, D., Kirkpatrick, G.J., 2008. Cell cycle behavior of laboratory and field populations of the Florida red tide dinoflagellate, *Karenia brevis*. Cont. Shelf Res. 28, 11–23.

Vargo, G.A., Heil, C.A., Ault, D.N., Neely, M.B., Murasko, S., Havens, J., Lester, K.M., Dixon, L.K., Merkt, R., Walsh, J., Weisberg, R., Steidinger, K.A., 2004. Four *Karenia brevis* blooms: a comparative analysis. In: Steidinger, K.A., Landsberg, J.H., Tomas, C.R., Vargo, G.A. (Eds.), Harmful Algae 2002. Florida Fish and Wildlife Conservation Commission, Florida Institute of Oceanography, and Intergovernmental Oceanographic Commission of UNESCO.